Title: OBSTRUCTIVE APNEAS IN A MOUSE MODEL OF CONGENITAL CENTRAL HYPOVENTILATION SYNDROME

Amélia Madani[1,*], Gabriel Pitollat[2,*], Eléonore Sizun[1], Laura Cardoit[2], Maud Ringot[1], Thomas Bourgeois[1], Nelina Ramanantsoa[1], Christophe Delclaux[1,3], Stéphane Dauger[1,4], Marie-Pia d'Ortho[1,5], Muriel Thoby-Brisson[2], Jorge Gallego[1], Boris Matrot[1]

Institutions

[1]Université de Paris, NeuroDiderot, Inserm, F-75019 Paris, France

[2]Université de Bordeaux, Institut de Neurosciences Cognitives et Intégratives d'Aquitaine, CNRS, Bordeaux, France

[3]Service d'Explorations Fonctionnelles Pédiatriques, AP-HP, Hôpital Robert Debré, F-75019 Paris, France

[4]Service de Médecine intensive-Réanimation pédiatriques, AP-HP, Hôpital Robert Debré, F-75019 Paris, France

[5]Service de Physiologie-Explorations Fonctionnelles, AP-HP, Hôpital Bichat, F-75018 Paris, France

* These authors contributed equally to this work.

Corresponding author: Jorge Gallego, NeuroDiderot, INSERM, Hôpital Robert Debré, 48 Bd Sérurier, 75019 Paris, France

E-mail: jorge.gallego@inserm.fr; Phone: (33) 140 031 975; FAX: (33) 140 031 920

Running title: Obstructive apneas in mice with *Phox2b* mutation

This article has an online data supplement, which is accessible from this issue's table of content online at www.atsjournals.org

Authors contributions

J.G., B.M., S.D., M.T.B and M.P.O. conceived and designed the study, and prepared the first draft of the manuscript. B.M. designed and produced the device for apnea measurement and

classification, T.B. validated this device and contributed to data analysis. A.M., E.S., M.R. acquired and analyzed respiratory measurements, N.R. generated the mutant mouse lines and supervised statistical analyses. G.P., L.C. and M.T.B., acquired and analyzed the histological and electrophysiological measurements. All authors contributed to the interpretation of the findings and critically revised the entire manuscript.

Sources of support

Institutional supports (Inserm and Université de Paris), Fonds de Recherche en Santé Respiratoire (F.R.S.R. grant to A.M.); Association Française du Syndrome d'Ondine (AFSO, grant to E.S.), Legs Poix (Chancellerie des Universités de Paris).

Running head: Central and obstructive apneas in *Phox2b*$^{27Ala/+}$ mice

Subject category: 15.1 Animal Models of Sleep Apnea

Total Word Count: 2937 words (<3500)

This article has an online data supplement, which is accessible from this issue's table of content online at www.atsjournals.org.

Abstract

Rationale: Congenital Central Hypoventilation Syndrome is characterized by life-threatening sleep hypoventilation, and is caused by *PHOX2B* gene mutations, most frequently the *PHOX2B*$^{27Ala/+}$ mutation. Patients require lifelong ventilatory support. It is unclear whether obstructive apneas are part of the syndrome.

Objectives: To determine whether *Phox2b*$^{27Ala/+}$ mice, which presented main symptoms of Congenital Central Hypoventilation Syndrome and died within hours after birth, also presented obstructive apneas and investigate potential underlying mechanisms.

Methods: Apneas were classified as central, obstructive or mixed by using an original system combining pneumotachography and laser detection of abdominal movement immediately after birth. Some respiratory nuclei involved in airway patency were analyzed by immunohistochemistry and electrophysiology in brainstem-spinal cord preparation.

Measurements and Main Results: The median (interquartile range) of obstructive apnea frequency was 2.3/min (1.5-3.3) in *Phox2b*$^{27Ala/+}$ pups versus 0.6/min (0.4-1.0) in wildtypes ($P < 0.0001$). Obstructive apnea duration was 2.7s (2.3-3.9) in *Phox2b*$^{27Ala/+}$ pups versus 1.7s (1.1-1.9) in wildtypes ($P < 0.0001$). Central and mixed apneas presented similar, significant differences. In *Phox2b*$^{27Ala/+}$ preparations, hypoglossal nucleus had fewer neurons ($P < 0.05$) and smaller size ($P < 0.01$), compared to wildtypes. Importantly, coordination of phrenic and hypoglossal activities was disrupted, as shown by the longer and variable delay of hypoglossal with respect to phrenic onset, compared to wildtypes ($P < 0.001$).

Conclusions: The *Phox2b*$^{27Ala/+}$ mutation predisposed pups not only to hypoventilation and central apneas, but also obstructive and mixed apneas likely due to hypoglossal dysgenesis. These results call for attention toward obstructive events in infants with Congenital Central Hypoventilation Syndrome.

Abstract word count: 250

Key words: Sleep apnea, Phox2b; phrenic nucleus, hypoglossal nucleus; airway obstruction.

Introduction

Congenital Central Hypoventilation Syndrome (CCHS) is an autosomal dominant disease whose incidence is unknown ranging from 1/50.000 to 1/200.000 live births (1). CCHS is characterized by loss of ventilatory chemosensitivity to hypercapnia and hypoxia, and life-threatening hypoventilation during sleep only or permanently in the most severe cases. The symptoms are generally noted at birth or during early infancy. Patients typically require lifelong positive pressure ventilation, at least nocturnal, via tracheostomy during early development, and then, through nasal or facial masks. CCHS is caused by heterozygous mutations in the paired-like homeobox 2B gene (*PHOX2B*) (2-4) that encodes a key transcription factor in the development of the autonomic nervous system (5). In 90% of cases, mutations are tri-nucleotide expansion mutations in *PHOX2B* leading to polyalanine expansions in the gene product (6). The most prevalent mutation is the 7-alanine expanded stretch ($PHOX2B^{27Ala/+}$). The non-polyalanine mutations (missense, frameshift, nonsense and stopcodon mutations) produce even more severe CCHS phenotypes, including the need for continuous ventilatory support, Hirschsprung disease and tumors.

Central apneas were commonly reported in CCHS patients and they were assigned to failure of central respiratory drive from the brainstem respiratory centers (7, 8). Obstructive apneas were occasionally reported in case or small-group studies (9-18) and were considered to require management in 50% of patients under one year (19). However, with rare exceptions (20), the studies of apneas in CCHS were conducted before the discovery of the disease-causing gene (2, 4) and possibly included heterogeneous patient groups. In current practice, obstructive apneas, if any, may remain unnoticed due to mechanical ventilation, which is generally used in a bi-level positive pressure mode (21). Thus, the question of whether obstructive disorders are part of CCHS is still open. This point may confuse ongoing research for pharmacological treatments.

Here, we analyzed whether the *Phox2b*$^{27Ala/+}$ mutation caused obstructive apneas in mice. Previous studies showed that the *Phox2b*$^{27Ala/+}$ mice presented main CCHS symptoms and died of respiratory arrest within hours after birth (22). Furthermore, the retrotrapezoid nucleus, a cluster of central chemoreceptors providing the major excitatory drive to breathing, was severely depleted (23, 24). Accordingly, apneas in *Phox2b*$^{27Ala/+}$ mice were assigned to retrotrapezoid nucleus agenesis and considered central. However, *Phox2b*$^{27Ala/+}$ mutation may also potentiate upper airway obstruction because *Phox2b*-expressing regions containing hypoglossal premotor neurons may be functionally impaired by the *Phox2b*$^{27Ala/+}$ mutation (25). On these bases, we hypothesized that *Phox2b*$^{27Ala/+}$ pups may present not only central, but also obstructive and mixed apneas. To test this, we developed an original method to classify apneas as central, obstructive and mixed in newborn mice, and we analyzed apneas in *Phox2b*$^{27Ala/+}$ pups and their neurological basis in late stage fetal *Phox2b*$^{27Ala/+}$ embryos.

Methods

Mice

We generated pups with the constitutive *Phox2b*$^{27Ala/+}$ mutation (22), hereafter *Phox2b*$^{27Ala/+}$ pups, and pups with the conditional, tissue-specific *Phox2b*$^{27Ala/+}$ mutation targeted to the retrotrapezoid nucleus (26), hereafter *Phox2b*$^{27Alacond/+}$ pups. See online supplement for the ethical approval and details on mutant generation and genotyping.

Pneumotachography

Breathing variables were measured using a pneumotachograph and a facemask combined into one single 3D printed part (Figure 1, A and B, hereafter termed "pneumotachometer"). The pneumotachometer was calibrated before each session. The flow signal was integrated for breath-by-breath measurement of tidal volume using a custom made software. We measured ventilation (V_E, calculated as f_R x V_T, ml/g/min), breathing frequency (f_R, number of

breaths/min), tidal volume (divided by body weight, V_T, ml/g) and apneas (detailed below). Breathing variables and apneas were analyzed over activity-free periods (based on video recordings) which were considered behavioral sleep. See details in the online supplement.

Laser detection of respiratory movements

Abdominal movements were detected using a laser distance sensor pointing radially at the lateral abdominal wall (Figure 1, A and B) to detect respiratory efforts during obstructive events. See details in the online supplement.

Apnea detection and classification

Apneas were scored as central, obstructive or mixed by adjusting the American Academy of Sleep Medicine recommendations (27) to newborn mice. An apnea was characterized by a > 90% decrement in peak inspiratory airflow for the duration of at least 0.90 s, which roughly corresponds to two breaths in neonatal mice. The classification into central, obstructive, and mixed apneas was performed by visual inspection of pneumotachometer and laser signals. An apnea was scored as central when no abdominal movement was present throughout the apnea, as obstructive when associated with continued abdominal movements, and as mixed when a central initial portion was followed by resumption of respiratory movements (Figure 1D).

Electrophysiology

Electrophysiological recordings of rhythmically organized respiration-related activities performed on isolated brainstem preparations harvested the day before birth (embryonic day (E) 18.5) have been performed as previously described (28). See details in the online supplement.

Protocol

Each pup was left with the mother for 15-20 min until the end of maternal care. Then, the pup was sexed, weighed and attached to the pneumotachograph inside a thermoregulated chamber (32°C). The snout was sealed into the facemask with polyether material (Impregum,

3M, France). Recordings were initiated within 100 min following delivery. Breathing variables were recorded for 60 min for apnea analyses (see the protocol in Supplemental Figure 2F) and prolonged beyond that period in *Phox2b*$^{27Ala/+}$ pups until terminal apnea to analyze gasping.

Statistics

For normally distributed data, we used two tailed t-tests and two-way ANOVAs, followed by Bonferroni's multiple comparisons test where appropriate. Non-normally distributed data were analyzed using Mann-Whitney test, followed by Dunn's post-hoc multiple comparisons test. Sex had no statistically significant effects in any analyses and will not be mentioned further. All analyses were performed using Prism 9 (GraphPad). *P*-values < 0.05 were considered significant.

Results

Baseline breathing and apnea time in *Phox2b*$^{27Ala/+}$ pups

Breathing pattern in *Phox2b*$^{27Ala/+}$ pups was characterized by significantly reduced ventilation and increased apnea time (irrespective of apnea types), compared to wildtypes (Table 1), confirming previous plethysmographic data (22). The lower V_E of *Phox2b*$^{27Ala/+}$ pups was mainly due to lower f_R. The V_E-response to hypercapnia was abolished in *Phox2b*$^{27Ala/+}$ pups, as previously shown (22) despite a small significant V_T-response (see Figure E1, A and B in the online data supplement).

Central, obstructive and mixed apneas in *Phox2b*$^{27Ala/+}$ pups

Compared to wildtypes, the *Phox2b*$^{27Ala/+}$ pups presented significantly more severe central, obstructive and mixed apneas, in terms of mean duration, frequency and total time (Figure 2). Total time of central apneas was longer (Figure 2A) due to both higher apnea frequencies (Figure 2B), and longer mean durations (Figure 2C). This result confirmed and extended previous claims that *Phox2b*$^{27Ala/+}$ mutation caused central apneas (22), based this

time on formal apnea classification. More importantly, the total time of obstructive apneas (never specifically investigated to date) was longer in *Phox2b*$^{27Ala/+}$ pups, compared to wildtypes (Figure 2A), due to higher apnea frequency (Figure 2B), and longer mean duration (Figure 2C). The comparison of mixed apneas between *Phox2b*$^{27Ala/+}$ pups and wildtypes yielded the same statistical results, as central and obstructive apneas (Figure 2, A-C)

Finally, the proportion of obstructive apneas (with respect to total number of apnea) was larger in *Phox2b*$^{27Ala/+}$ pups, compared to wildtype pups (29% ± 14 versus 23% ± 13, respectively, $P < 0.05$), and the time proportion of obstructive apneas (with respect to total time spent in apnea) was also longer in *Phox2b*$^{27Ala/+}$ pups (31% ± 14 versus 22% ± 13, respectively, $P < 0.001$).

Obstructed gasping in *Phox2b*$^{27Ala/+}$ newborn mice

We then examined the possibility that airway obstruction contributed to the death of *Phox2b*$^{27Ala/+}$ pups in a subsample of mutant pups (n=45) in which respiratory recording was maintained until respiratory arrest. The occurrence of gasps is illustrated in Figure 3. The initial period during which breathing was variably affected (Figure 3 A and B), was followed by a period of disorganized breathing interspersed with gasps, characterized by large and brief respiratory efforts accompanied by large inspirations (Figure 3C). Some of these large abdominal movements did not generate inspiration, indicating obstructed gasps (Figure 3D). In the 3-min period preceding respiratory arrest 25 out of 45 (55%) pups produced such obstructed gasps.

The role of retrotrapezoid neuronal loss in apneas

We investigated whether the obstructive pattern of *Phox2b*$^{27Ala/+}$ pups was due to the agenesis of retrotrapezoid nucleus, which was the unique neuroanatomical defect reported to date in *Phox2b*$^{27Ala/+}$ pups. To this end, we replicated the main study in conditional knock-in, tissue-specific mice, in which the *Phox2b*$^{27Ala/+}$ mutation was targeted to retrotrapezoid nucleus

region. These mutant pups hereafter designated *Phox2b*$^{27Alacond/+}$ pups, previously analyzed from two-day of postnatal age, survived normally without apneas, despite the agenesis of retrotrapezoid nucleus and the consequent loss of CO_2-chemosensitivity (26). Here, we showed that *Phox2b*$^{27Alacond/+}$ pups (within 100 min after birth) had lower V_E mainly due to lower f_R values, and longer total apnea time (irrespective of apnea types) compared to wildtypes (Table E2). The ventilatory response to CO_2 was practically abolished in *Phox2b*$^{27Alacond/+}$ pups (Supplemental Figure E3) confirming retrotrapezoid neuronal loss. The sole loss of retrotrapezoid neurons in *Phox2b*$^{27Alacond/+}$ pups not only increased frequency and total time of central apneas, but it also increased the mean duration of obstructive apneas, compared to wildtypes (Figure 4, A-C). No statistical comparison was done between *Phox2b*$^{27Ala/+}$ and *Phox2b*$^{27Alacond/+}$ pups, since these data were collected in two different studies, but a rough examination of apnea characteristics in the two mutants clearly indicated that the apneic phenotype was much more severe in *Phox2b*$^{27Ala/+}$, compared to *Phox2b*$^{27Alacond/+}$ pups. Thus, the sole loss of the retrotrapezoid nucleus promoted central apneas and aggravated obstructive apnea in *Phox2b*$^{27Alacond/+}$ pups, but it could not account for the dramatic apneic phenotype of *Phox2b*$^{27Ala/+}$ pups.

Dysgenesis and dysfunction of hypoglossal nucleus in *Phox2b*$^{27Ala/+}$ newborn mice

Because obstructive and mixed apneas in *Phox2b*$^{27Ala/+}$ pups were not mainly ascribable to retrotrapezoid agenesis, we examined the hypoglossal nucleus, which is the main groups of motoneurons involved in the control of upper airway muscles (29). In *Phox2b*$^{27Ala/+}$ pups, the hypoglossal nucleus presented an abnormal anatomy (Figure 5A and B) characterized by a smaller perimeter (Figure 5C), a smaller surface (Figure 5D), and fewer neurons (Figure 5E), despite normal rostrocaudal extension (Figure 5F) and neuroanatomical location (Figure 5G).

To examine whether the function of hypoglossal nucleus was affected by the *Phox2b*$^{27Ala/+}$ mutation, we recorded spontaneous hypoglossal and phrenic nerve activity in

E18.5 isolated brainstem-spinal cord preparations, that retains respiratory-related phrenic and hypoglossal activities *in vitro*. Electrophysiological monitoring of hypoglossal nucleus (Figure 6A) revealed significant functional disorders in *Phox2b*$^{27Ala/+}$ preparations (Figure 6). Specifically, burst frequency was significantly reduced in *Phox2b*$^{27Ala/+}$ preparations compared to wildtypes (Figure 6B), in line with their reduced breathing frequency *in vivo,* and rise time of bursts was also reduced without significantly affecting burst duration (Figure 6, C-E). Most importantly, the joint analysis of hypoglossal and phrenic activities showed a marked loss of coordination of these activities (Figure 6). Specifically, the mutant preparations presented a longer and more variable delay of hypoglossal onset with respect to phrenic onset, which contrasted with the roughly synchronous activities of wildtype preparations (Figure 6, F and G). The large intra-individual variability of the delay between hypoglossal and phrenic burst onset (Figure 6F) was observed in all *Phox2b*$^{27Ala/+}$ preparations, and further pointed toward impaired coordination of these activities.

Discussion

We showed that, compared to wildtypes, newborn mice bearing the *Phox2b*$^{27Ala/+}$ constitutive mutation showed abnormally high amounts of not only central but also obstructive and mixed apneas. These latter tended to be longer than central apneas. Furthermore, terminal apnea was frequently preceded by obstructed gasps, suggesting a causal or aggravating role in some pups. The obstructive phenotype of *Phox2b*$^{27Ala/+}$ was ascribed at least partly to dysgenesis and dysfunction of the hypoglossal nucleus, which is critical to maintenance of upper airway patency.

Methodology for apnea detection and classification in newborn mice

Here we conducted the first study discriminating apneas per types (central, obstructive and mixed) in newborn mice, thanks to an original method that combined a built-in precision

pneumotachometer and an ultra-sensitive laser distance sensor. Previous attempts to classify apnea in newborn rodents were developed in 7-day old rats using electromyography electrodes implanted in respiratory muscles under anesthesia (30). This approach was not applicable in the present study due the short lifetime (70% died within three hours after delivery) and high vulnerability to anesthesia of *Phox2b*$^{27Ala/+}$ mutants (31). Despite our efforts to adjust the facemask to the pups' morphology, the orofacial contact with the mask may have influenced sleep-wake states and breathing. To control for this effect, we strictly discarded all periods of gross body movements based on video recordings to exclusively retain behavioral sleep periods. However, we cannot discard that some periods of quiet wakefulness were included in apnea analysis, irrespective of genotype. A further limitation of our study is that no attempt was made to discriminate sleep states, because, at this early postnatal stage, this would have required the invasive measure of nuchal EMG (32). Thus, the sleep state dependence pattern of apnea characteristics was not investigated. Previous studies in five-day old mice indicated that active sleep reached approximately 80% of sleep time, in line with human data (32), which suggested that the apneic pattern described here mainly reflected those that developed during active sleep. Despite these limitations, the present methodology allowed the classification of apneas in an infant mouse model of CCHS, with possible applications to any other rodent model of sleep disordered breathing in infants.

Apnea profile in *Phox2b*$^{27Ala/+}$ newborn mice

As noted, apneas in *Phox2b*$^{27Ala/+}$ pups were previously ascribed to loss of CO_2-driven excitatory input to respiratory rhythm generator by the retrotrapezoid nucleus, and considered as central. The main result of the present study was that the *Phox2b*$^{27Ala/+}$ mutation caused not only central apneas, but also obstructive and mixed apneas. On the one hand, central apneas were more frequent than obstructive and mixed apneas, and expected to produce more numerous hypoxia-reoxygenation sequences, which are considered the main cause of apnea-

related morbidity. On the other hand, obstructive and mixed apneas were significantly longer than central apneas, and thus potentially associated to larger decreases in heart rate and oxygen saturation (33). Furthermore, the co-occurrence of obstructive events and terminal apnea suggested that obstructive events precipitated terminal apnea and death in numerous *Phox2b*$^{27Ala/+}$ pups. Taken together, these result supported that obstructive events caused by the *Phox2b*$^{27Ala/+}$ mutation may seriously affect morbidity and mortality in the neonatal period.

Neurological mechanisms of obstructive apneas in *Phox2b*$^{27Ala/+}$ newborn mice

The hypoglossal motor nucleus innervates the muscles of the tongue, and therefore withdrawal of excitatory drives of hypoglossal motoneurons is a common cause of obstructive apneas (29). The dysgenesis of the hypoglossal nucleus found in the present study is a novel result. In previous studies, neuroanatomical defects were sought primarily in *Phox2b*-expressing structures, leading to the discovery of retrotrapezoid nucleus agenesis (22), leaving aside the hypoglossal nucleus, which does not depend on *Phox2b* for its development (25). The dysgenesis of hypoglossal nucleus thus showed that the *Phox2b*$^{27Ala/+}$ mutation elicited non-cell-autonomous mechanisms affecting respiratory networks. Such mechanisms were only reported to date in newborn mice with a non-polyalanine repeat mutation (the frameshift *Phox2BΔ8* mutation), that presented dysfunctional preBötzinger complex, a non-*Phox2b* dependent brainstem site that is responsible for respiratory rhythmogenesis (34). Taken together, these results widen the spectrum of respiratory control disorders possibly caused by *Phox2b* mutations.

The neuroanatomical defects of hypoglossal nucleus were associated with functional defects, the most significant one being the uncoupling of hypoglossal and phrenic nerve activities. In physiological conditions, the hypoglossal nucleus tends to burst synchronously with the phrenic nerve to exert tonic input to the upper airway dilator muscle motor neurons and prevent airway collapse during inspiratory depression (35, 36). Here, as a rule, the onset of

hypoglossal discharge was less well coordinated respect to diaphragmatic activity in *Phox2b*$^{27Ala/+}$ pups, in contrast to wildtypes. This suggested that, *in vivo*, the inspiratory negative pressure in *Phox2b*$^{27Ala/+}$ pups was not counteracted by tonic activity of upper airway muscles at least during the initial part of inspiration, thus increasing propensity to obstructive events. In addition to the likely impact of hypoglossal dysfunction on obstructive events, we also showed that the sole loss of retrotrapezoid nucleus generated longer obstructive apneas (as shown in *Phox2b*$^{27Alacond/+}$ pups). This result provided *in vivo* support to the notion that the retrotrapezoid nucleus contributes to the control of genioglossus muscle activity (37, 38). Thus, hypoglossal and retrotrapezoidal defects probably combined their effects to aggravate obstructive apneas in *Phox2b*$^{27Ala/+}$ pups. However, we cannot discard that hypoglossal activity was also affected by dysfunction of numerous regions containing hypoglossal premotor neurons expressing *Phox2b* and possibly affected by the mutation (25).

Clinical relevance

The high incidence of not only central, but also obstructive and mixed apneas in *Phox2b*$^{27Ala/+}$ newborn mice suggested that airway patency disorders also occur in infants with CCHS but remain unnoticed due to permanent tracheostomy, and/or positive pressure ventilation. Also, the present study suggested that, if observed, obstructive events should not rule out the diagnostic of CCHS. This study also suggested that obstructive events in patients with CCHS need attention in the perspective of future treatment research, which, to date, was mainly oriented toward respiratory stimulants (39-41). This study also sheds new light on the neurobiology and neurodevelopment of pharyngeal muscle control with potential translation towards pharmacotherapy targeting pharyngeal patency and obstructive sleep apnea syndromes.

Conclusion

This study demonstrated that the *Phox2b*$^{27Ala/+}$ mutation, which is the most frequent cause of CCHS, produced not only central, but also obstructive and mixed apnea in newborn mice.

The obstructive disorders were assigned at least partly, to dysfunction of the hypoglossal nucleus, a non-*Phox2b* expressing structure, combined with those of disrupted input from retrotrapezoid nucleus. These results broaden the spectrum of neuroanatomical and neurofunctional disorders caused by *Phox2b* mutations, and call for increased attention toward obstructive events in infants with CCHS.

ACKNOWLEDGEMENTS

We are deeply indebted to Florian Brunet and Sebastien Lanteri for their contribution to apnea detection device, to Fabien Duverger for his contribution to pneumotachometer design, and to Pr. Chih-Wei Hsu for providing 3D scans of newborn mouse.

DISCLOSURE STATEMENT

- Financial Disclosure: none.
- Non-financial Disclosure: none

References

1. Bardanzellu F, Pintus MC, Fanos V, Marcialis MA. Neonatal congenital central hypoventilation syndrome: Why we should not sleep on it. Literature review of forty-two neonatal onset cases. *Curr Pediatr Rev* 2019;15:139-153.
2. Amiel J, Laudier B, Attie-Bitach T, Trang H, de Pontual L, Gener B, Trochet D, Etchevers H, Ray P, Simonneau M, Vekemans M, Munnich A, Gaultier C, Lyonnet S. Polyalanine expansion and frameshift mutations of the paired-like homeobox gene phox2b in congenital central hypoventilation syndrome. *Nat Genet* 2003;33:459-461.
3. Matera I, Bachetti T, Puppo F, Di Duca M, Morandi F, Casiraghi G, Cilio M, Hennekam R, Hofstra R, Schöber J, Ravazzolo R, Ottonello G, Ceccherini I. Phox2b mutations and polyalanine expansions corellate with the severity of the respiratory phenotype and associated symptoms in both congenital and late onset central hypoventilation syndrome. *J Med Genet* 2004;41:373-380.
4. Weese-Mayer DE, Berry-Kravis EM, Zhou L, Maher BS, Silvestri JM, Curran ME, Marazita ML. Idiopathic congenital central hypoventilation syndrome: Analysis of genes pertinent to early autonomic nervous system embryologic development and identification of mutations in phox2b. *Am J Med Genet* 2003;123A:267-278.
5. Brunet JF, Pattyn A. Phox2 genes - from patterning to connectivity. *Curr Opin Genet Dev* 2002;12:435-440.
6. Weese-Mayer DE, Berry-Kravis EM, Ceccherini I, Keens TG, Loghmanee DA, Trang H. An official ats clinical policy statement: Congenital central hypoventilation syndrome: Genetic basis, diagnosis, and management. *Am J Respir Crit Care Med* 2010;181:626-644.
7. Huang J, Colrain IM, Panitch HB, Tapia IE, Schwartz MS, Samuel J, Pepe M, Bandla P, Bradford R, Mosse YP, Maris JM, Marcus CL. Effect of sleep stage on breathing in children with central hypoventilation. *J Appl Physiol (1985)* 2008;105:44-53.
8. Cielo C, Marcus CL. Central hypoventilation syndromes. *Sleep Med Clin* 2014;9:105-118.
9. Weese-Mayer DE, Berry-Kravis EM, Zhou L. Adult identified with congenital central hypoventilation syndrome--mutation in phox2b gene and late-onset chs. *Am J Respir Crit Care Med* 2005;171:88.
10. Bygarski E, Paterson M, Lemire EG. Extreme intra-familial variability of congenital central hypoventilation syndrome: A case series. *J Med Case Rep* 2013;7:117.
11. Lamon T, Pontier S, Tetu L, Riviere D, Didier A. [the congenital central hypoventilation syndrome (cchs): A late presentation]. *Rev Mal Respir* 2012;29:426-429.
12. Katwa U, D'Gama AM, Qualls AE, Donovan LM, Heffernan J, Shi J, Agrawal PB. Atypical presentations associated with non-polyalanine repeat phox2b mutations. *Am J Med Genet A* 2018;176:1627-1631.
13. Kurz H, Sterniste W, Dremsek P. Resolution of obstructive sleep apnea syndrome after adenoidectomy in congenital central hypoventilation syndrome. *Pediatr Pulmonol* 1999;27:341-346.
14. Amimoto Y, Okada K, Nakano H, Sasaki A, Hayasaka K, Odajima H. A case of congenital central hypoventilation syndrome with a novel mutation of the phox2b gene presenting as central sleep apnea. *J Clin Sleep Med* 2014;10:327-329.
15. Byers HM, Chen M, Gelfand AS, Ong B, Jendras M, Glass IA. Expanding the phenotype of congenital central hypoventilation syndrome impacts management decisions. *Am J Med Genet A* 2018;176:1398-1404.

16. Silvestri JM, Chen ML, Weese-Mayer DE, McQuitty JM, Carveth HJ, Nielson DW, Borowitz D, Cerny F. Idiopathic congenital central hypoventilation syndrome: The next generation. *Am J Med Genet* 2002;112:46-50.
17. Emanuel H, Rennie K, Macdonald K, Yadav A, Mosquera RA. Screening children with a family history of central congenital hypoventilation syndrome. *Case Rep Pediatr* 2020;2020:2713606.
18. Mahmoud M, Bryan Y, Gunter J, Kreeger RN, Sadhasivam S. Anesthetic implications of undiagnosed late onset central hypoventilation syndrome in a child: From elective tonsillectomy to tracheostomy. *Paediatr Anaesth* 2007;17:1001-1005.
19. Olson TS, Woodson GE, Heldt GP. Upper airway function in ondine's curse. *Arch Otolaryngol Head Neck Surg* 1992;118:310-312.
20. Kasi AS, Kun SS, Keens TG, Perez IA. Adult with phox2b mutation and late-onset congenital central hypoventilation syndrome. *J Clin Sleep Med* 2018;14:2079-2081.
21. Chen ML, Keens TG. Congenital central hypoventilation syndrome: Not just another rare disorder. *Paediatr Respir Rev* 2004;5:182-189.
22. Dubreuil V, Ramanantsoa N, Trochet D, Vaubourg V, Amiel J, Gallego J, Brunet JF, Goridis C. A human mutation in phox2b causes lack of co2 chemosensitivity, fatal central apnea, and specific loss of parafacial neurons. *Proc Natl Acad Sci U S A* 2008;105:1067-1072.
23. Guyenet PG, Stornetta RL, Souza G, Abbott SBG, Shi Y, Bayliss DA. The retrotrapezoid nucleus: Central chemoreceptor and regulator of breathing automaticity. *Trends Neurosci* 2019;42:807-824.
24. Guyenet PG, Bayliss DA, Stornetta RL, Ludwig MG, Kumar NN, Shi Y, Burke PG, Kanbar R, Basting TM, Holloway BB, Wenker IC. Proton detection and breathing regulation by the retrotrapezoid nucleus. *J Physiol* 2016;594:1529-1551.
25. Kang BJ, Chang DA, Mackay DD, West GH, Moreira TS, Takakura AC, Gwilt JM, Guyenet PG, Stornetta RL. Central nervous system distribution of the transcription factor phox2b in the adult rat. *The Journal of comparative neurology* 2007;503:627-641.
26. Ramanantsoa N, Hirsch MR, Thoby-Brisson M, Dubreuil V, Bouvier J, Ruffault PL, Matrot B, Fortin G, Brunet JF, Gallego J, Goridis C. Breathing without co(2) chemosensitivity in conditional phox2b mutants. *J Neurosci* 2011;31:12880-12888.
27. Berry R, Brook R, Gamaldo C, Harding S, Lloyd R, Quan S, Troester M, Vaughn B. The aasm manual for the scoring of sleep and associated events: Rules, terminology, and technical specifications.; 2017.
28. Dubois CJ, Cardoit L, Schwarz V, Markkanen M, Airaksinen MS, Uvarov P, Simmers J, Thoby-Brisson M. Role of the k(+)-cl(-) cotransporter kcc2a isoform in mammalian respiration at birth. *eNeuro* 2018;5.
29. Horner RL. Emerging principles and neural substrates underlying tonic sleep-state-dependent influences on respiratory motor activity. *Philos Trans R Soc Lond B Biol Sci* 2009;364:2553-2564.
30. Kidder IJ, Mudery JA, Bailey EF. Neural drive to respiratory muscles in the spontaneously breathingrat pup. *Respiratory Physiology & Neurobiology* 2014;202:64-70.
31. Bourgeois T, Ringot M, Ramanantsoa N, Matrot B, Dauger S, Delclaux C, Gallego J. Breathing under anesthesia: A key role for the retrotrapezoid nucleus revealed by conditional phox2b mutant mice. *Anesthesiology* 2019;130:995-1006.
32. Durand E, Dauger S, Pattyn A, Gaultier C, Goridis C, Gallego J. Sleep-disordered breathing in newborn mice heterozygous for the transcription factor phox2b. *Am J Respir Crit Care Med* 2005;172:238-243.

33. Muttitt SC, Finer NN, Tierney AJ, Rossmann J. Neonatal apnea: Diagnosis by nurse versus computer. *Pediatrics* 1988;82:713-720.
34. Alzate-Correa D, Mei-Ling Liu J, Jones M, Silva TM, Alves MJ, Burke E, Zuniga J, Kaya B, Zaza G, Aslan MT, Blackburn J, Shimada MY, Fernandes-Junior SA, Baer LA, Stanford KI, Kempton A, Smith S, Szujewski CC, Silbaugh A, Viemari JC, Takakura AC, Garcia AJ, 3rd, Moreira TS, Czeisler CM, Otero JJ. Neonatal apneic phenotype in a murine congenital central hypoventilation syndrome model is induced through non-cell autonomous developmental mechanisms. *Brain Pathol* 2020.
35. Chamberlin NL, Eikermann M, Fassbender P, White DP, Malhotra A. Genioglossus premotoneurons and the negative pressure reflex in rats. *J Physiol* 2007;579:515-526.
36. Horner RL, Hughes SW, Malhotra A. State-dependent and reflex drives to the upper airway: Basic physiology with clinical implications. *J Appl Physiol (1985)* 2014;116:325-336.
37. Silva JN, Lucena EV, Silva TM, Damasceno RS, Takakura AC, Moreira TS. Inhibition of the pontine kolliker-fuse nucleus reduces genioglossal activity elicited by stimulation of the retrotrapezoid chemoreceptor neurons. *Neuroscience* 2016;328:9-21.
38. Dutschmann M, Herbert H. The kolliker-fuse nucleus gates the postinspiratory phase of the respiratory cycle to control inspiratory off-switch and upper airway resistance in rat. *Eur J Neurosci* 2006;24:1071-1084.
39. Nattie E. Ondine undone. *N Engl J Med* 2015;373:573-575.
40. Weese-Mayer DE, Silvestri JM, Menzies LJ, Morrow-Kenny AS, Hunt CE, Hauptman SA. Congenital central hypoventilation syndrome: Diagnosis, management, and long-term outcome in thirty-two children. *J Pediatr* 1992;120:381-387.
41. Di Lascio S, Benfante R, Cardani S, Fornasari D. Research advances on therapeutic approaches to congenital central hypoventilation syndrome (cchs). *Front Neurosci* 2020;14:615666.

FIGURE LEGENDS

FIGURE 1: Experimental setup for detection and classification of central, obstructive and mixed apneas in newborn mice. A: (Technical drawing). The pneumotachometer incorporating the Fleisch pneumotachograph and the facial mask was affixed on the pup's snout and sealed with Impregum (3M, France). A flow through the mask (20 mL/min^{-1}) prevented rebreathing. A laser profilometer detected abdominal movements in a 2 mm x 0.5 mm zone (black rectangle). B: (Frame extracted from video) showing the facemask and the laser beam. The whole setup was placed in a thermoregulated chamber (not shown). C: Individual traces of volume, obtained by integrating the flow signal from the pneumotachograph (upper trace) and movements by laser profilometry (lower trace) of a wildtype pup. D: Examples of central (no flow, no movements), obstructive (no flow, abdominal movements) and mixed (no flow, abdominal movement at the end of apnea) in a *Phox2b*$^{27Ala/+}$ pup. E: Graphical representation of the experimental protocol. After 5 min baseline breathing, each pup was exposed to 8% CO_2 in air, and then back to air for 50 min recording.

FIGURE 2: The *Phox2b*$^{27Ala/+}$ mutation aggravated central, obstructive and mixed apneas in *newborn* pups compared to wildtypes. Apneas were quantified by Total time (A) calculated as the ratio of total apnea durations divided by recording time after exclusion of activity periods, apnea frequency (B), and apnea mean duration (C). Undetermined apneas represented less than 2% of total apnea time in either group and were not represented. The high interindividual variability of apnea characteristics in mutants is in keeping with that of their lifetime, which ranged from a few minutes to 24 hours, and also with that of clinical symptoms of patients with CCHS. Lines and whiskers in boxplots represent the medians, the interquartile ranges, and the minimum and maximum values. * : $P = 0.0129$; *** : $P < 0.0001$.

FIGURE 3: Examples of unobstructed and obstructed terminal gasps in a *Phox2b*$^{27Ala/+}$ pup. A: Slow, regular breathing. B: Breathing interspersed with apneas. C: Irregular breathing

with apneas and an unobstructed gasp accompanied by abdominal expansion (arrows). D: Long obstructive apnea followed by two obstructed gasps (arrows). The four sequences (A, B, C and D) were recorded in the same *Phox2b*$^{27Ala/+}$ pup after 3h02, 4h15, 4h22 and 4h52 of recording, respectively.

FIGURE 4: The conditional, tissue-specific *Phox2b*$^{27Alacond/+}$ mutation aggravated central and obstructive apneas, compared to wildtypes. Apneas were scored within 100-min following birth. Apneas were quantified by Total time (A) calculated as the ratio of total apnea durations divided by recording time after exclusion of activity periods, frequency (B), and mean duration (C) of apneas. Lines and whiskers in boxplots represent the medians, the interquartile ranges, and the minimum and maximum values. In comparison with *Phox2b*$^{27Ala/+}$ pups (Figure 2), the apneic phenotype of *Phox2b*$^{27Alacond/+}$ was much less severe. *: $P < 0.05$; ***: $P = 0.0006$

FIGURE 5. Abnormal anatomy of the hypoglossal nucleus in the Phox2b$^{27Ala/+}$ mutant. (*A*) Schematic representations of an isolated brainstem preparation (left), a coronal brainstem slice (right, top) and a sagittal brainstem slice (right, bottom) with the corresponding position of the RTN (red shading), the preBötzinger complex (orange shading) and the hypoglossal (XII) nucleus (gray shading). The double-headed violet arrows indicate the coronal (1) and sagittal (2) plans of section. The violet rectangles delimit the areas shown in B. (*B*) Immunostainings against Islet1,2 (green) in 30µm thick brainstem coronal (top) and sagittal (bottom) slices obtained from embryonic day 18.5 WT and *Phox2b*$^{27Ala/+}$ embryos. White lines delimit the XII nuclei. (*C, D, E, F, G*) Histograms showing the overall mean (±SEM) for XII nucleus perimeter (*C*) and surface (*D*), the number of neurons per XII nucleus (*E*), the rostro-caudal extension (*F*) and the position relative to the caudal end of the VII nucleus (*G*) of the XII nucleus measured from WT (green) and *Phox2b*$^{27Ala/+}$ (blue) animals. The number of preparations analyzed is indicated for each bar graph. Values are given as mean ± SEM. *P <0.05, **P < 0.01 indicate

significant differences (t-test), ns indicates no statistical difference. In the mutant the XII nucleus is smaller, contains less neurons but with the same rostro-caudal extension and position relative to the VII nucleus. C4: phrenic rootlet, RTN: retrotrapezoïd nucleus, preBötC: preBötzinger complex, VII: facial nucleus, XII: hypoglossal nucleus, WT: wild type.

FIGURE 6. The hypoglossal nerve is functional but its bursts shape and its coordination with the phrenic nerve activity are changed in the *Phox2b*$^{27Ala/+}$ mutant. (*A*) Left, Schematic representation of an isolated brainstem preparation with the set up used for simultaneous electrophysiological monitoring of hypoglossal and phrenic nerve activities. Right, Representative rectified and integrated (Int) simultaneous recordings from hypoglossal (XII) and phrenic (C4) ventral roots in *in vitro* preparations obtained from a wildtype (WT, green traces) and a mutant (*Phox2b*$^{27Ala/+}$, blue traces) mice. (*B*) Graph showing the mean XII burst frequency measured from 12 WT (green) and 9 *Phox2b*$^{27Ala/+}$ (blue) preparations. (*C*) Superimposed XII bursts and average trace (thick trace) taken from a representative recording obtained from a WT (n = 9 bursts, green) and a *Phox2b*$^{27Ala/+}$ (n = 11 bursts, blue) preparations. (*D*) and (*E*) Graphs showing the mean burst rise time and mean burst duration obtained from XII bursts in WT (n = 120 events, green) and *Phox2b*$^{27Ala/+}$ (n = 90 events, blue) recordings. (*F*) Superimposition of hypoglossal (top) and phrenic (bottom) spontaneous bursts of motor activity measured in a WT (green) and a *Phox2b*$^{27Ala/+}$ (blue) preparations. The dotted lines indicate the mean onset of the XII bursts. Note that the coordination between phrenic and hypoglossal bursts is affected in the *Phox2b*$^{27Ala/+}$ preparations. (*G*) Boxplot with whiskers (min to max) representing the delay between phrenic and hypoglossal bursts. Phrenic bursts initiate earlier than XII bursts in the *Phox2b*$^{27Ala/+}$ preparations over a wider range of values. Values are given as mean ± SEM. $^{**}P < 0.01$, $^{***}P < 0.001$ indicate significant differences (Mann-Whitney t-test), ns indicates no statistical difference.

TABLE 1

Variables	Wildtype n = 48	*Phox2b*$^{27Ala/+}$ n = 36	*P* value
Weight (g)	1.33 ± 0.09	1.28 ± 0.1	0.007
Movement time (s/min)	24 ± 7	15 ± 8	< 0.001
f_R (breaths/min)	98 ± 18	46 ± 19	< 0.001
V_T (mL/g x 10^{-3})	6.7 ± 0.9	6.3 ± 1.4	0.104
V_E (mL/min/g)	0.65 ± 0.13	0.29 ± 0.16	< 0.001
Apnea time (s/min)	7.22 ± 4.60	26.67 ± 12.79	< 0.001

Table 1: Baseline breathing variables and ventilatory response to hypercapnia in constitutive *Phox2b*$^{27Ala/+}$ newborn mice confirmed conformity with CCHS phenotype: hypoventilation, apnea, and absence of ventilatory response to hypercania. Data were collected within 100 min following birth. Movement time was expressed in s per min of recording time. f_R: breathing frequency; V_T: tidal volume; V_E: mean ventilation. Apnea time was expressed in s per min of movement-free time (assimilated to sleep), and calculated irrespective of apnea type. *P* values: comparison between mutants and wildtypes using t-tests. Values are means ± SD.

TABLE 2

Variables	Wildtype n = 62	*Phox2b*$^{27Alacond/+}$ n = 58	*P* value
Weight (g)	1.31 ± 0.12	1.35 ± 0.10	0.0198
Movement time (s/min)	27 ± 10	24 ± 8	0.049
f_R (breaths/min)	97 ± 28	79 ± 24	< 0.001
V_T (mL/g x 10^{-3})	6.6 ± 0.9	6.3 ± 0.8	0.079
V_E (mL/min/g)	0.64 ± 0.19	0.49 ± 0.14	< 0.001
Apnea time (s/min)	8.08 ± 5.92	11.34 ± 8.62	0.017

Table 2: Baseline breathing variables in conditional tissue-specific *Phox2b*$^{27Alacond/+}$ newborn mice and their wildtype controls. Data were collected within 100 min following birth. Movement time was expressed in s per min of recording time. f_R: breathing frequency; V_T: tidal volume; V_E: mean ventilation. Apnea time (in s per min of movement-free time) was calculated irrespective of apnea type. *P* values: comparison between mutants and wildtypes using t-tests. Values are means ± SD.

FIGURE 1

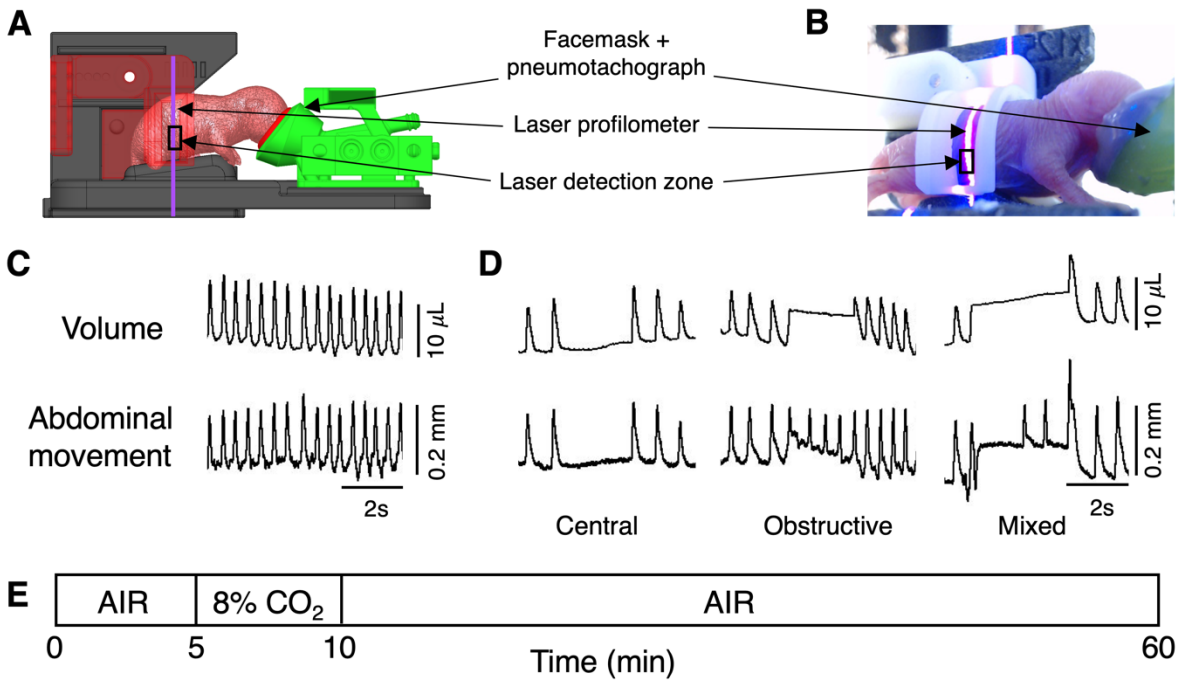
A
B
Facemask +
pneumotachograph
Laser profilometer
Laser detection zone
C
Volume
10 µL
Abdominal
movement
0.2 mm
2s
D
10 µL
0.2 mm
2s
Central
Obstructive
Mixed
E
AIR
8% CO2
AIR
0
5
10
60
Time (min)

FIGURE 2

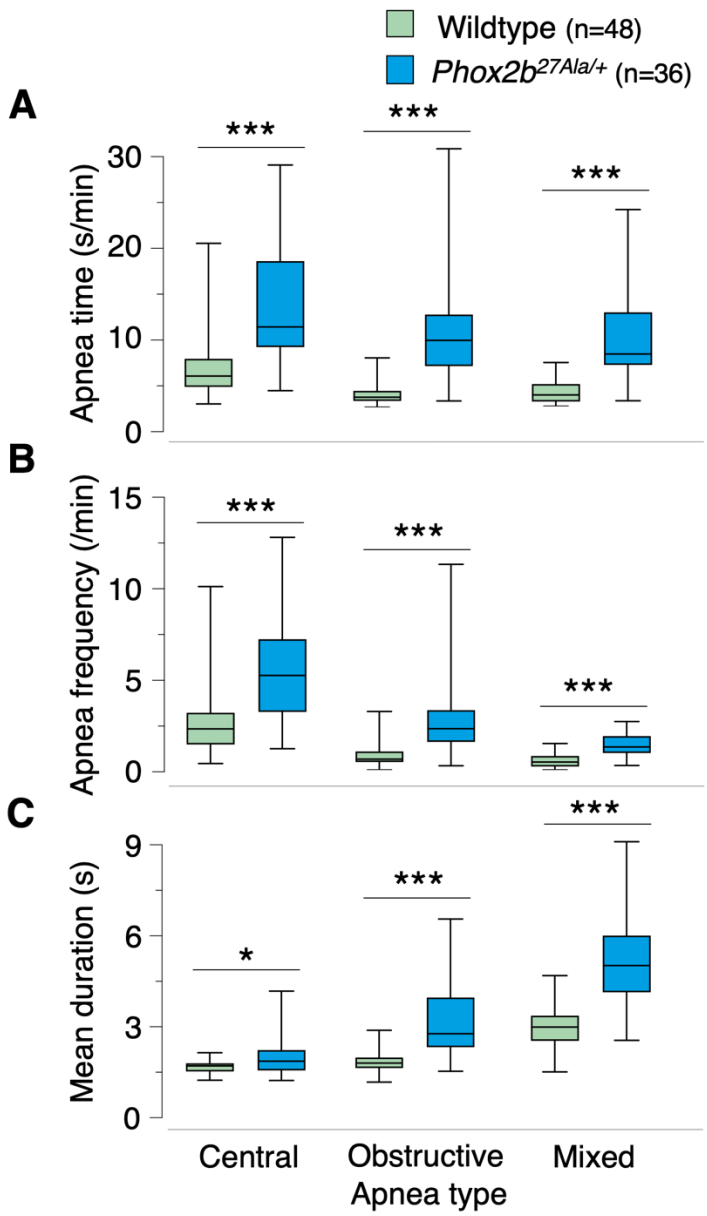
Wildtype (n=48)
Phox2b27Ala/+ (n=36)
A
B
C
Apnea time (s/min)
Apnea frequency (/min)
Mean duration (s)
***
*
Central
Obstructive
Mixed
Apnea type

FIGURE 3

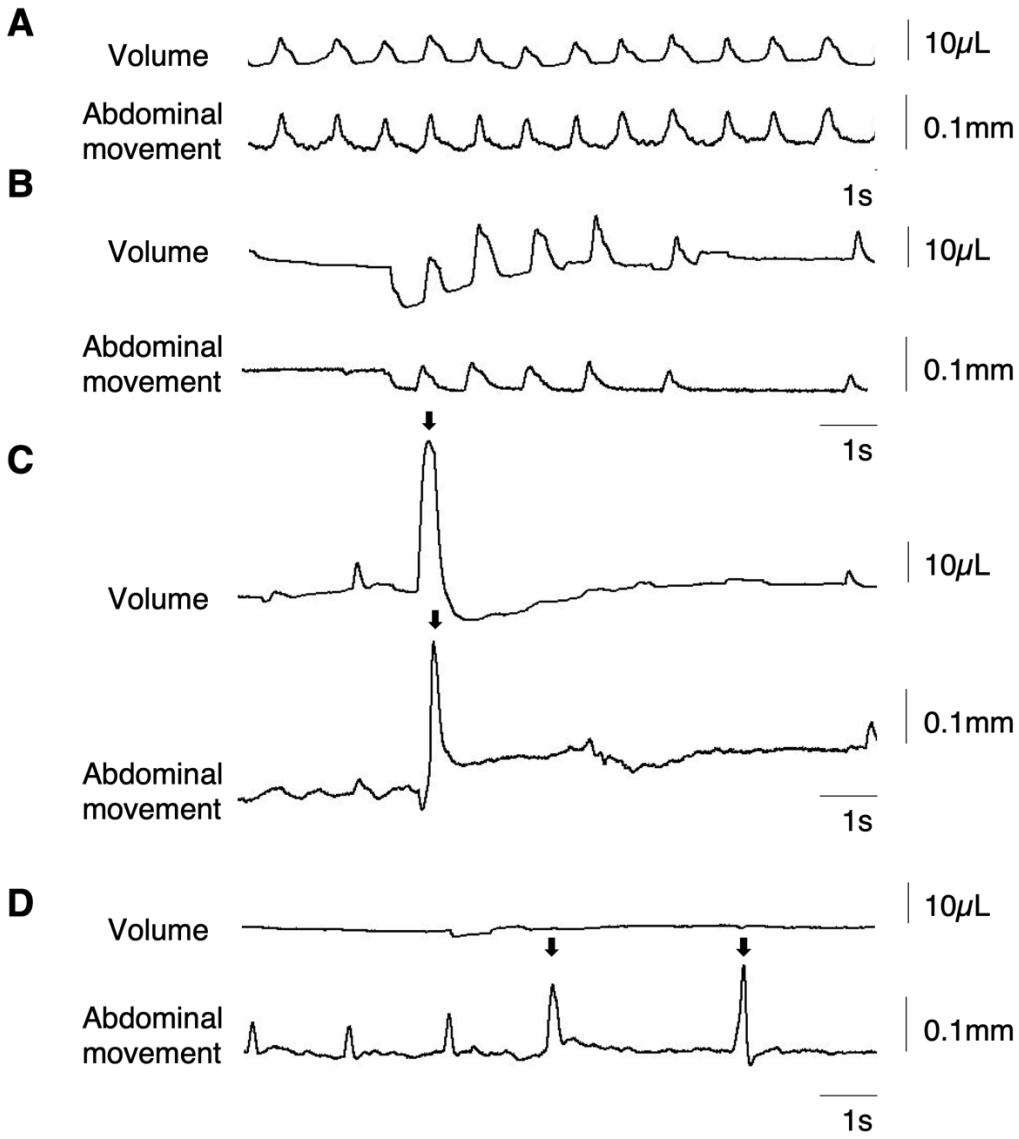
A
Volume
10μL
Abdominal movement
0.1mm
1s
B
Volume
10μL
Abdominal movement
0.1mm
1s
C
Volume
10μL
Abdominal movement
0.1mm
1s
D
Volume
10μL
Abdominal movement
0.1mm
1s

FIGURE 4

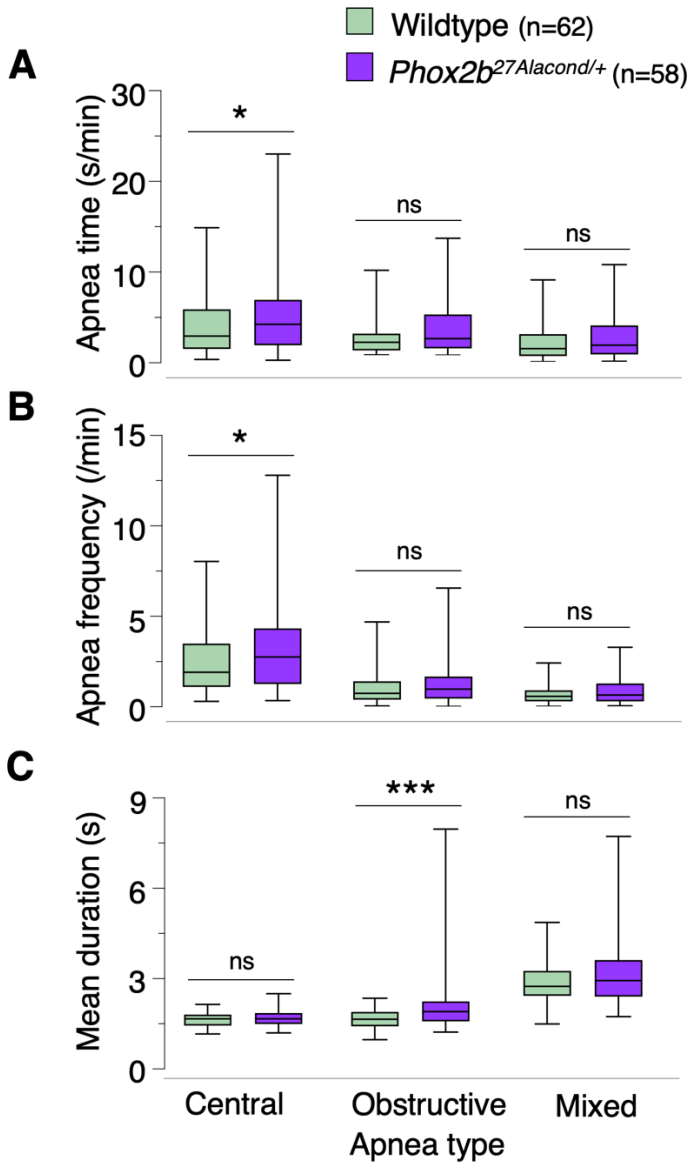
Wildtype (n=62)
Phox2b27Alacond/+ (n=58)
A
Apnea time (s/min)
30
20
10
0
*
ns
ns
B
Apnea frequency (/min)
15
10
5
0
*
ns
ns
C
Mean duration (s)
9
6
3
0
ns
***
ns
Central
Obstructive
Mixed
Apnea type

FIGURE 5

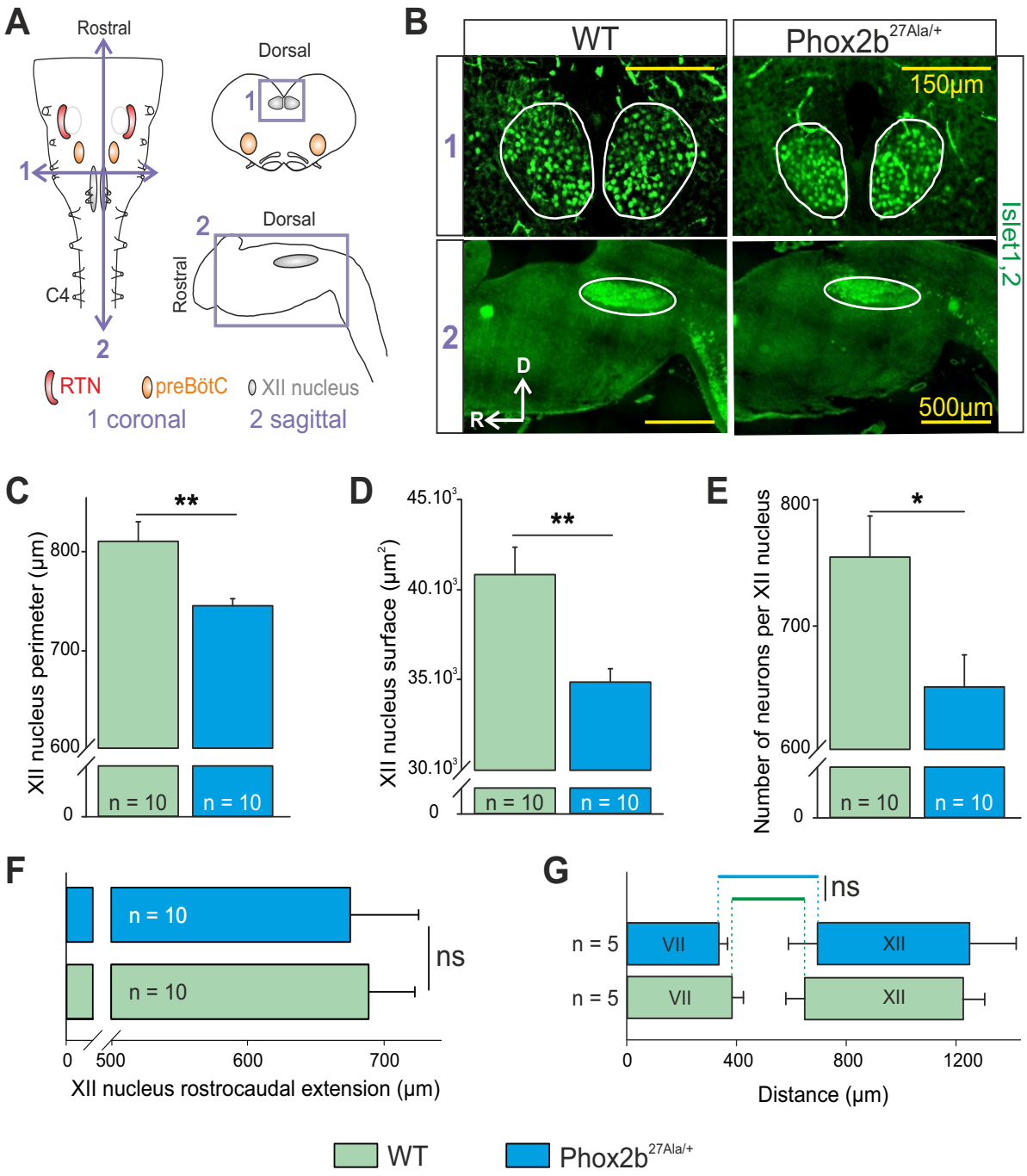
A
Rostral
Dorsal
1
C4
2
Dorsal
Rostral
RTN
preBötC
XII nucleus
1 coronal
2 sagittal
B
WT
Phox2b27Ala/+
150µm
500µm
Islet1,2
D
R
C
XII nucleus perimeter (µm)
800
700
600
0
**
n = 10
n = 10
D
XII nucleus surface (µm2)
45.10³
40.10³
35.10³
30.10³
0
**
n = 10
n = 10
E
Number of neurons per XII nucleus
800
700
600
0
*
n = 10
n = 10
F
n = 10
n = 10
ns
0
500
600
700
XII nucleus rostrocaudal extension (µm)
G
ns
n = 5
n = 5
VII
VII
XII
XII
0
400
800
1200
Distance (µm)
WT
Phox2b27Ala/+

FIGURE 6

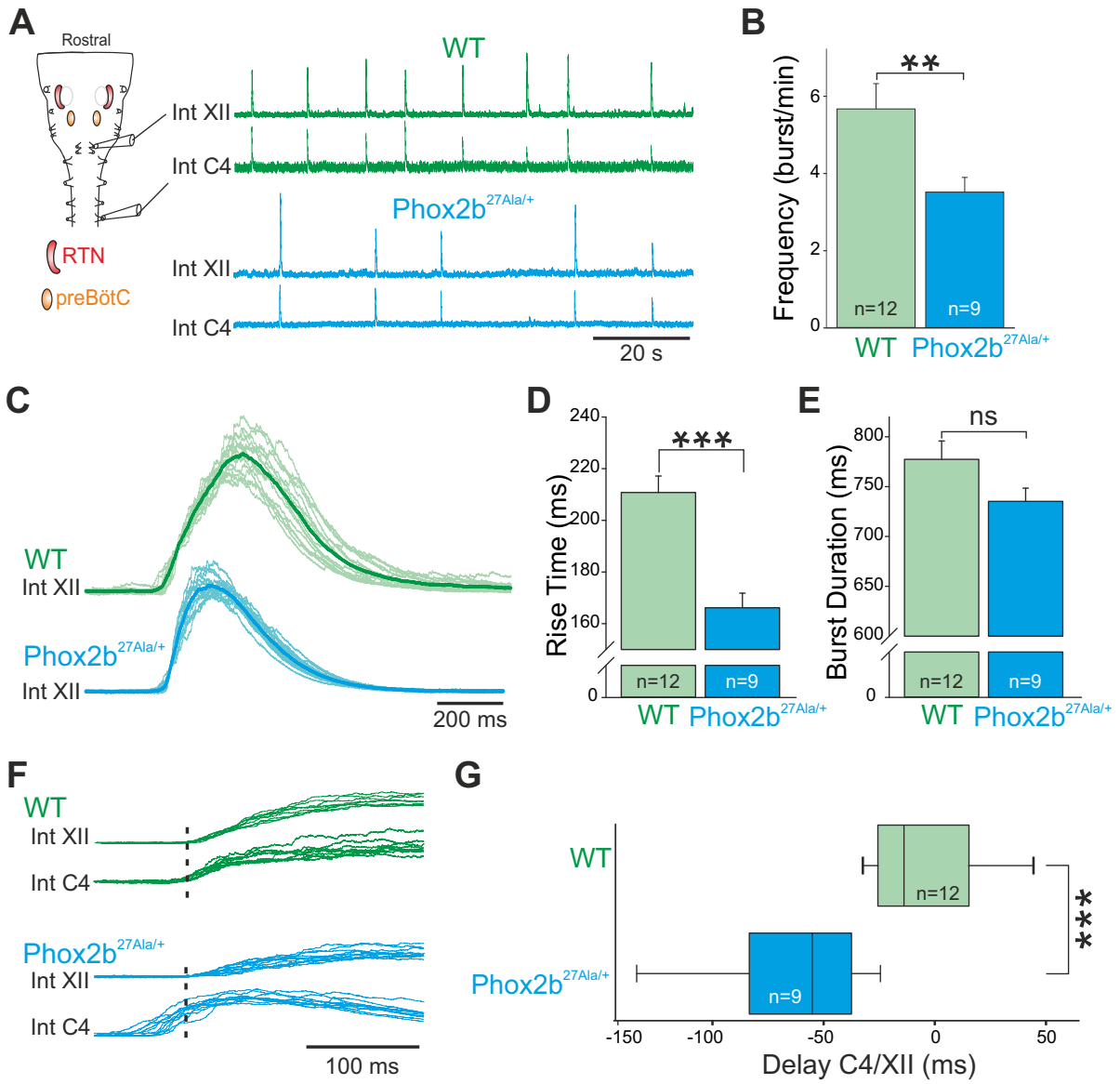
A
Rostral
RTN
preBötC
WT
Int XII
Int C4
Phox2b27Ala/+
Int XII
Int C4
20 s
B
Frequency (burst/min)
**
n=12
n=9
WT
Phox2b27Ala/+
C
WT
Int XII
Phox2b27Ala/+
Int XII
200 ms
D
Rise Time (ms)
***
n=12
n=9
WT
Phox2b27Ala/+
E
Burst Duration (ms)
ns
n=12
n=9
WT
Phox2b27Ala/+
F
WT
Int XII
Int C4
Phox2b27Ala/+
Int XII
Int C4
100 ms
G
WT
n=12
Phox2b27Ala/+
n=9
***
-150
-100
-50
0
50
Delay C4/XII (ms)